View metadata, citation and similar papers at core.ac.uk
brought to you by CORE
provided by Springer - Publisher Connector

Nanoscale Res Lett (2010) 5:1236–1239
DOI 10.1007/s11671-010-9625-y

NANO PERSPECTIVES

Size Effect on Failure of Pre-stretched Free-Standing Nanomembranes

Rong Long · Chung-Yuen Hui · Wenlong Cheng · Michael J. Campolongo · Dan Luo

Received: 28 February 2010 / Accepted: 29 April 2010 / Published online: 15 May 2010
© The Author(s) 2010. This article is published with open access at Springerlink.com

Abstract Free-standing nanomembranes are two-dimensional materials with nanometer thickness but can have macroscopic lateral dimensions. We develop a fracture model to evaluate a pre-stretched free standing circular ultrathin nanomembrane and establish a relation between the energy release rate of a circumferential interface crack and the pre-strain in the membrane. Our results demonstrate that detachment cannot occur when the radius of the membrane is smaller than a critical size. This critical radius is inversely proportional to the Young's modulus and square of the pre-strain of the membrane.

Keywords Free standing membrane · Pre-stretch · Size effect · Energy release rate

Introduction

Free-standing ultrathin nanomembranes are a new class of two-dimensional materials that possess nanoscale thickness across macroscopic dimensions. Such nanomembranes are not only ultra-lightweight but also robust and flexible. It has been reported that elastic moduli of ultrathin nanomembranes can be 1–10 GPa with ultimate strengths of up to 100 MPa [1–6]. These striking properties of free-standing nanomembranes have resulted in a broad spectrum of applications in separation, sensing, biomedicine and energy harvesting [7–10].

These free-standing nanomembranes are usually subjected to residual tensions induced during formation or by thermal mismatch. As a result, they may detach from the suspending micro-holes and lose their functionality [11, 12]. Experiments have demonstrated that smaller free standing membranes are structurally and thermally more stable than larger ones [9, 10]. This size dependence is also observed by Cheng et al. [11] who fabricated free standing membranes composed of highly ordered arrays of gold nanoparticles linked by single strand DNA molecules. Briefly, these membranes are formed using the following process: first, droplets of a solution consisting of 13 nm diameter gold nanoparticles capped with 5′-thiolated single strand DNA (ssDNA) is dried on a thin silicon nitrate substrate with micron size holes in it. Satellite micro-droplets were formed and trapped in these microholes due to pinning of contact lines by the hole edges. As solvent evaporated, these pinned satellite micro-droplets thinned and formed monolayer nanoparticle membranes. Pre-tensions were built up on the membranes during this drying stage. It was found that these membranes tended to detach from the edges of larger microholes, but not smaller ones (Fig. 1).

Model

We propose a model to understand the size effect on the detachment of membranes due to pre-stretch. Micro-holes used in the experiments are usually rectangular or circular.

R. Long (✉) · C.-Y. Hui
Sibley School of Mechanical and Aerospace Engineering, Cornell University, Ithaca, NY 14853, USA
e-mail: rl267@cornell.edu

W. Cheng
Department of Chemical Engineering, Monash University, Clayton, VIC 3800, Australia

M. J. Campolongo · D. Luo
Departmen of Biological and Environmental Engineering, Cornell University, Ithaca, NY 14853, USA

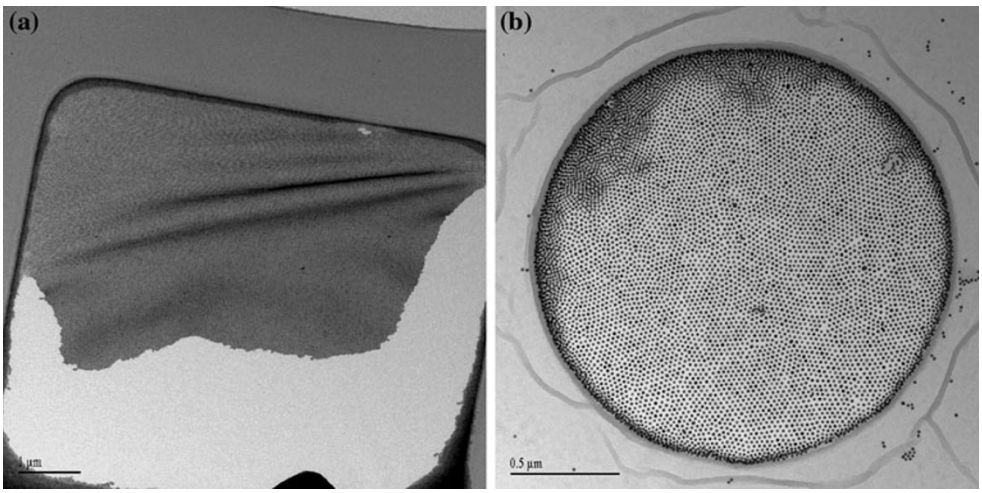

Fig. 1 **a** A free standing membrane is partially detached from a 7.5 μm × 6.5 μm rectangular hole. **b** A free standing membrane is fully attached to a circular hole with diameter of 2 μm

For simplicity, we assume that the micro-holes are circular with radius R. The thin substrate with micro-holes is assumed to be rigid. Let $h \ll R$ denote the thickness of the membrane. For a circular membrane without defect, the pre-stretch is equi-biaxial and is spatially uniform. Since the out of plane stresses are identically zero, the membrane deforms under plane stress conditions. With respect to a polar coordinate system (r, θ) with origin at the center of the circular membrane, the non-zero pre-strains in a membrane without defect are $\varepsilon_{rr} = \varepsilon_{\theta\theta} \equiv \varepsilon$, where $\varepsilon_{rr}, \varepsilon_{\theta\theta}$ are the axial and hoop strains, respectively. This equi-biaxial stretch state can be achieved mechanically by imposing a radial displacement of εR on the circumference of the membrane. The strain energy density of the pre-stretched membrane is $E\varepsilon^2/(1-\nu)$, where E and ν are the Young's modulus and the Poisson's ratio of the membrane, respectively. The total elastic strain energy Γ of the membrane without defect is

$$\Gamma = \frac{E\varepsilon^2}{(1-\nu)} \cdot \pi R^2 h. \tag{1}$$

A simple scaling argument shows why membranes with larger radius are more likely to fail. Specifically, we envision two failure modes: adhesive or cohesive. In adhesive failure, a crack grows along the edge of the micro-hole. In cohesive failure, crack growth occurs inside a region of the membrane that is adjacent to the interface (e.g. see Fig. 1a). To quantify these failures, we define W as the energy required to detach or break a unit area of membrane in the interface region. This region includes the edge of the micro-hole as well as a thin layer of membrane adjacent to it. If adhesive failure occurs, W is identified as adhesion energy per unit area between the membrane and the substrate, while in cohesive failure, W is the facture toughness of the membrane. The energy needed to detach the *entire* membrane from the edge is $2\pi RhW$. The elastic energy stored in the membrane Γ will not be large enough to detach the entire membrane if

$$W \cdot 2\pi Rh > \Gamma. \tag{2}$$

Using (1), the inequality in (2) can be rewritten as

$$\frac{E\varepsilon^2 R}{2(1-\nu)W} < 1. \tag{3}$$

Equation (3) shows why sheets over smaller holes (smaller R) is less likely to fail. This conclusion is also valid for non-circular shaped micro-holes; in this case R should be replaced by the characteristic length of the micro-hole.

The above argument is too simplistic since it assumes that detachment occurs on the *entire* interface, whereas in reality, only partial detachment is observed (Fig. 1a). We ask a more general question: suppose there is a defect on or near the interface between the membrane and the micro-hole edge, will this defect grow? If the defect grows, elastic energy is released locally to debond or break the membrane and part of the membrane is relaxed. To model this process, we consider an interface crack of length $a < 2\pi R$ as shown in Fig. 2. The surface of this crack is traction-free whereas the rest of the membrane circumference is subjected to a radial displacement of εR. According to fracture mechanics [13], a necessary condition for the growth of this interface crack is

$$G \geq W, \tag{4}$$

where G is the energy release rate of the crack. Energy release rate is the elastic energy per unit film thickness that

would be released if the crack were to extend by a unit distance along the interface. In this analysis, deviation of the crack trajectory from the interface (e.g. in cohesive failure) is assumed to be small so that the energy release rate G can be computed by assuming the crack is right on the interface.

Linearity and dimensional argument show that

$$G = E\varepsilon^2 R f(\theta_o, \nu) \qquad \theta_o \equiv a/2R, \tag{5}$$

where f is an unknown dimensionless function of θ_o ($0 \le \theta_o \le \pi$), the half angle sustained by the interface crack (see Fig. 2). We will call $f(\theta_o, \nu) \equiv G/(E\varepsilon^2 R)$ the normalized energy release rate. Its behavior for small cracks ($\theta_o \ll 1$) can be found using a simple argument. In this limit, the crack can be viewed as a straight crack with length a lying on the interface between the lower half plane (circular membrane) and the upper half plane (rigid substrate). The crack is loaded by a hydrostatic tension $\sigma = E\varepsilon/(1-\nu)$ at infinity. The energy release rate for this geometry is:

$$G = \frac{\sigma^2 \pi a}{4E}\omega(\nu) = \frac{E\varepsilon^2 \pi a}{4}\frac{\omega(\nu)}{(1-\nu)^2}, \tag{6}$$

where the dimensionless numerical factor ω in (6) depends only on the membrane's Poisson's ratio, and is an order 1 quantity [14]. Equation (6) shows that $f(\theta_o, \nu)$ is a linear function of θ_o for small cracks. Applying the crack growth criterion (4) using (6), we found small defects ($a/R \ll 1$) with

$$\theta_o < \frac{2(1-\nu)^2 W}{\pi\omega E\varepsilon^2 R}, \tag{7}$$

will not grow.

For longer cracks, growth is possible. To study this possibility, we note that (5) and (6) imply that the normalized energy release rate $f(\theta_o \to 0, \nu) \to 0$. In addition, since the strain energy of the membrane goes to zero as $a \to 2\pi R$ (or $\theta_o \to \pi$), the energy release rate is expected to vanish in this "long" crack limit. This explains why complete detachment does not occur. The fact that f vanishes at both end points (0 and π) means that f must have an interior maximum $f^* > 0$ at some $\theta_o^* \in (0, \pi)$. The existence of this maximum and the crack growth criterion (4) imply that no defect can grow if

$$W > E\varepsilon^2 R f^*, \tag{8}$$

where f^* is a numerical constant which depends only on the Poisson's ratio of the membrane.

The normalized energy release rate f and its maximum f^* are determined numerically using finite element method. Details of the finite element calculation are given in Appendix A. Figure 3 plots the normalized energy release rate $f(\theta_o, \nu)$ against θ_o for $\nu = 0$, 0.1, 1/3, 0.4 and 0.49. The energy release rate increases linearly θ_o for small cracks as predicted by (7), reaches a maximum at θ_o^* and then decreases rapidly to zero. The fact that the energy release rate decreases to zero after θ_o^* implies that the interface crack will always be arrested before it can de-cohere the entire membrane, consistent with experimental observation that the interface crack eventually arrests before the complete detachment of membrane can take place (Fig. 1). According to (8), irrespective of the size of a defect, it cannot grow if $W/(E\varepsilon^2 R) > f^*$. Values of f^* for different Poisson's ratio ν can be approximated by $f^* = 4.26\nu^2 + 0.49\nu + 0.92$ with $\nu \in [0, 0.5]$. This result suggests that membrane detachment can be prevented when the membrane radius R is smaller than a critical radius R_c:

$$R < R_c \equiv \frac{W}{E\varepsilon^2(4.26\nu^2 + 0.49\nu + 0.92)}. \tag{9}$$

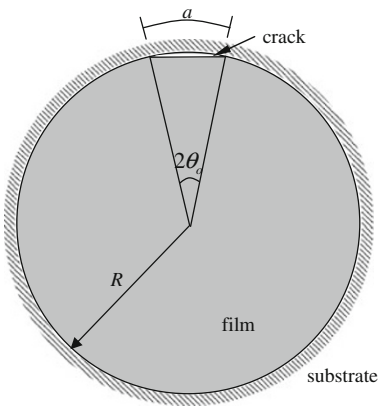

Fig. 2 Pre-stretched thin membrane with an interface crack of length a. The membrane is subjected to a radial displacement of εR at its circumference outside the crack

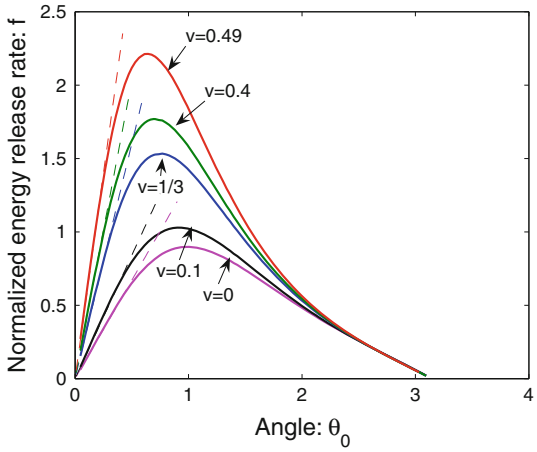

Fig. 3 Normalized energy release rate $f(\theta_o, \nu) \equiv G/(E\varepsilon^2 R)$ versus $\theta_o = a/2R$ for Poisson's ratio $\nu = 0$, 0.1, 1/3, 0.4 and 0.49. The dashed lines show that energy release rate increases linearly with crack length when the crack is small

Equation (9) also implies that stiff membranes are easier to detach than soft membranes for the same W and ε. This result is consistent with our preliminary experimental results. In these experiments, the stiffness of the membrane can be tuned by varying the length of the DNA molecules attached to the gold particles [11]. However, more data is needed to confirm this result.

Our experimental observations suggest that R_c is in the range of 1–4 μm. The Young's modulus E of a typical membrane is reported to be about 6.5 GPa [11]. Assuming v is 1/3, the pre-strain ε is estimated to be 0.12%. This estimate is based on the initial slope of the force–displacement curve of indentation tests [11], where we have assumed that the force–displacement curve is controlled by the pre-tension for small deflections and approximated the indenter as a point load. There is no direct measurement of W. Using the values of R_c, E, ε and v listed above, W is estimated to be 15–50 mJ/m^2, which is consistent with the strength of van der Waals interaction [15].

Conclusion

In summary, a fracture mechanics model is used to explain why small free-standing membranes are more resistant to detachment. We show that detachment can be prevented by making the membrane smaller for a given pre-strain and W, which is consistent with our experimental observations. A useful expression for critical radius of the membrane is obtained and may guide future design of free-standing membrane systems.

Acknowledgments C.Y. Hui and R. Long are supported by a grant from the Department of Energy (DE-FG02-07ER46463). W. Cheng, M. Campolongo and D. Luo are partially supported by NYSTAR and the NSF CAREER award (grant number: 0547330).

Open Access This article is distributed under the terms of the Creative Commons Attribution Noncommercial License which permits any noncommercial use, distribution, and reproduction in any medium, provided the original author(s) and source are credited.

Appendix A

Numerical calculations were carried out using ABAQUS, a finite element software [16]. Radial displacement of εR was imposed on the edge of the circular membrane outside the crack while the crack face was left traction free. A typical mesh consisted of approximately 4,000 plane stress four-node quadrilateral elements. Finer mesh was used near the crack tip. The total strain energy of the system Γ can be found for any normalized crack length θ_o, and the energy release rate can be computed according to

$$G = \frac{\Gamma(\theta_o) - \Gamma(\theta_o + \Delta\theta_o)}{2hR\Delta\theta_o}, \tag{10}$$

where $\Delta\theta_o$ is a small increment in normalized crack length. We started the simulation with a very small crack and gradually increased its length. The calculation is tedious since each crack length increment requires remeshing and change of boundary conditions. This process was automated using a PYTHON script. The energy release rate was also computed using the J-integral option in ABAQUS. We found practically no difference between the two methods.

References

1. W. Cheng, M.J. Campolongo, S.J. Tan, D. Luo, Nano Today **4**, 482–493 (2009)
2. C.Y. Jiang, B.M. Rybak, S. Markutsya, P.E. Kladitis, V.V. Tsukruk, Appl Phys Lett **86**, 121912 (2005)
3. K.E. Mueggenburg, X.M. Lin, R.H. Goldsmith, H. Jaeger, Nat Mater **6**, 656–660 (2007)
4. S. Markutsya, C. Jiang, Y. Pikus, V.V. Tsukruk, Adv Func Mater **15**(771), 771 (2005)
5. A. Fery, F. Dubreuil, H. Möhwald, New J Phys **6**, 18 (2004)
6. O.I. Vinogradova, J Phys Condens Matt **16**, R1105 (2004)
7. C. Jiang, S. Markutsya, Y. Pikus, V.V. Tsukruk, Nat Mat **3**, 721 (2004)
8. B.C.H. Steele, A. Heinzel, Nature **414**, 345 (2001)
9. C.D. Baertsch, K.F. Jensen, J.L. Hertz, H.L. Tuller, S.T. Vengallatore, S.M. Spearing, M.A. Schmidt, J Mater Res **19**, 2604 (2004)
10. L.X. Tiefenauer, A. Studer, Biointerphases **3**, FA74 (2008)
11. W. Cheng, M.J. Campolongo, J.J. Cha, S.J. Tan, C.C. Umbach, D.A. Muller, D. Luo, Nat Mater **8**, 519 (2009)
12. J. Jin, Y. Wakayama, X. Peng, I. Ichinose, Nat mater **6**, 686 (2007)
13. T.L. Anderson, *Fracture mechanics: fundamentals and applications*, 3rd edn. (CRC Press, Boca Raton, 2005)
14. J.R. Rice, J Appl Mech **55**, 99 (1988)
15. J. Israelachvili, *Intermolecular & surface forces*, 2nd edn. (Academic Press, London, 1992)
16. ABAQUS Version 6.7 Dassault Systemes Simulia Corp., Providence, RI, USA